9-Aryl-Phenalenones: Bioinspired Thermally Reversible Photochromic Compounds for Photoswitching Applications in the Pico- to Milliseconds Range

Authors: Roger Bresolí-Obach,[a,b] Walter A. Massad,[a,c] Abasi Abudulimu,[d] Larry Lüer,[d,e] Cristina Flors,[d] Javier G. Luis,[f,g] Laura I. Rosquete,[f,g] Teresa A. Grillo,[f,g] Ommid Anamimoghadam,[h] Götz Bucher,[h,*] Santi Nonell[a,*]

[a] Institut Químic de Sarrià, Universitat Ramon Llull, Via Augusta 390, E-08017, Barcelona, Catalunya, Spain

[b] Currently: Laboratory for Photochemistry and Spectroscopy, MIP, Department of Chemistry, Katholieke Universiteit Leuven Celestijnenlaan 200F, 3001 Heverlee, Leuven, Belgium.

[c] Instituto para el Desarrollo Agroindustrial y de la Salud (IDAS). CONICET – UNRC., Depto. De Química – FCEF-QyN - Universidad Nacional de Río Cuarto, Rio Cuarto, Argentina.

[d] IMDEA Nanociencia, C/ Faraday 9, E-28049 Madrid, Spain

[e] Institute of Materials for Electronics and Energy Technology (i-MEET), Friedrich-Alexander University Erlangen-Nürnberg, Martensstraße 7, 91058 Erlangen, Germany

[f] Instituto Universitario de Bio-Orgánica ‘‘Antonio González’’, Universidad de La Laguna, Avda. Astrofísico Fco. Sán-chez 2, La Laguna, E-38206, Tenerife, Canary Islands, Spain.

[g] Departamento de Química Orgánica, Facultad de Farmacia, Universidad de La Laguna, Avda. Astrofísico Fco. Sánchez s/n, La Laguna, E-38206, Tenerife, Canary Islands, Spain.

[h] School of Chemistry, University of Glasgow, Joseph-Black-Building, University Avenue, Glasgow G12 8QQ, UK.

Corresponding e-mail: Santi.nonell@iqs.edu, Goetz.Bucher@glasgow.ac.uk

Abstract

Ultrafast photochromic molecules are being actively investigated to meet the demand for fast optical switching systems. Inspired on the irreversible cyclization of 9-phenylphenalenone plant metabolites to yield highly-coloured naphthoxanthenes for the purpose of defense against pathogens, aryl-substituted phenalenones have been developed that undergo a similar but reversible photochromic reaction. The lifetime of the naphthoxanthene photoisomer spans nine orders of magnitude, ranging from tens of picoseconds to tens of milliseconds depending on the electronic properties of the 9-aryl group.

Keywords: β-phenyl quenching • photochromic • phenalenone • chromene • photoswitch

1. Introduction

Nature has evolved a rich repertoire of materials and systems that can reversibly adjust their structure and properties in response to environmental stimuli.[1] Light as a stimulus presents the advantages of high spatio-temporal control as well as insensitivity to environmental factors and can be applied in an external, non-invasive, and residue-free fashion.[2] Molecules with photochemically switchable properties play a crucial role in a wide range of modern applications, including functional molecules, their assemblies, materials used for data storage, and logic operations in optoelectronic devices, as well as biotechnological and pharmacological applications, especially for optogenetics and imaging.[3-7] Thus, photochromic compounds capable of reversibly photoisomerizing between at least two different (meta)-stable isomers with markedly different properties, e.g., geometry, spectroscopic signature, polarity, magnetic state, spatial ordering, or surface tension,[8-12] are the subject of current interest for fast optical switching applications.[13] T-type photoswitches, where the photochemically-generated isomers revert thermally to the initial form, are of advantage for some applications because no additional photons are needed to bring the system back to its original state.[14-21]

Previous work from our laboratories has revealed that 9-phenylphenalenones (9PPNs) can undergo reversible photocyclization upon light excitation, a process termed β-phenyl quenching (BPQ).[22-24] The closed-ring structure, a naphthoxanthene (NX), is unstable due to the loss of aromaticity and spontaneously reverts to the starting material (Scheme 1 top). Photocyclization of 9PPNs is at the heart of a mechanism used by plants to defend themselves from pathogens.[25-28] 9PPNs produce reactive oxygen species when exposed to UV and blue light[29-32] and produce secondary metabolites capable of absorbing light at longer wavelengths (Scheme 1 bottom).[33-37] The structural similarity between these metabolites and the NXs produced in the cyclization of 9PPNS, suggests a common mechanism of production. A major difference is the superior stability of the natural counterparts conferred by the rearomatization of the NX form by hydroxy-oxo tautomerization. In the course of our investigations on bioinspired phenalenone derivatives,[38,39] we discovered that it is possible to alter the stability of the closed NX form by modifying the substituents in the 9-phenyl group. In this work, we show that replacing the phenyl substituent

by heteroaryl groups (Scheme 1 middle) results in a dramatic variation of the NX lifetime over nine orders of magnitude.

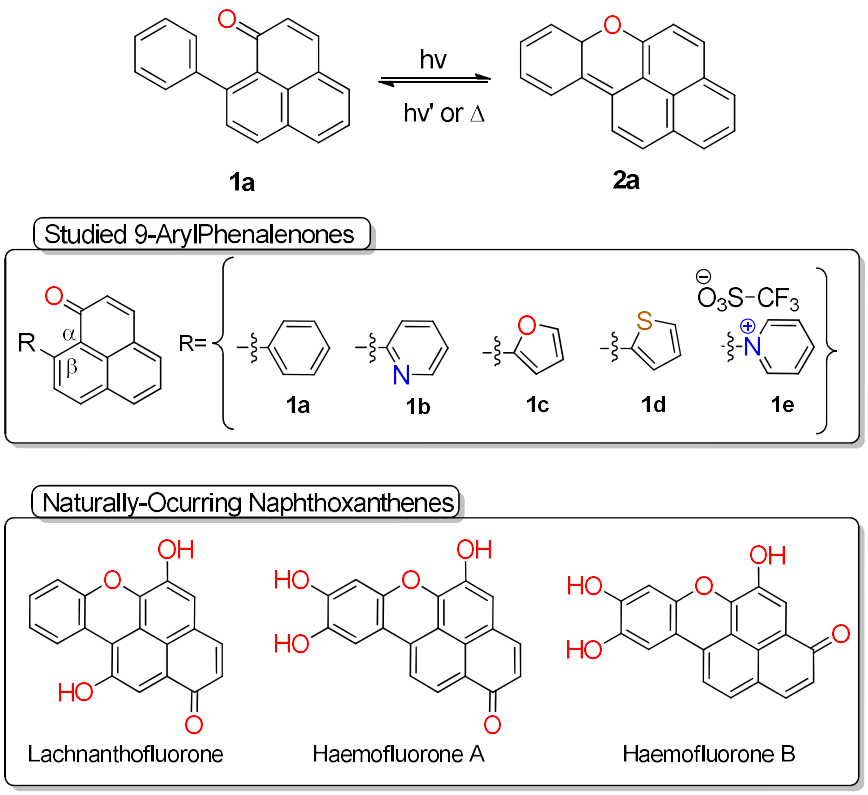

Scheme 1. Top: Reversible ring closure and opening in 9-phenyl-phenalenone.[22,23] Middle: Structure of the 9-arylphenalenones studied in this work. Bottom: Naturally-occurring naphthoxanthenes derived from 9PPNs.

2. Results and discussion

2.1 Spectroscopic experimental results

All the 9-arylphenalenones **1a-1e** absorb in the ultraviolet and blue regions with a tail that extends to 500 nm (Figure 1, panels A-D and Figure 2A). Nanosecond laser flash photolysis of **1a-1d** in argon-saturated solutions produced long-lived transients (Figure 1, panels E-H), which were assigned to the corresponding NXs **2a**-**2d** following the protocols of our previous work:[23,40] (i) The experimental and calculated maxima in the UV-Vis spectra are in excellent agreement (515 vs 524 nm for **2b**, 430 vs 449 nm for **2c**, and 460 vs 474 nm for **2d**; Figure 1, panels I-L and Figures S1-S3,

respectively). The difference is below 5% for all compounds, which falls within the error range expected for the theory level used. Of note, in these time-resolved spectra we can observe both the disappearance of **2a**-**2d** (λ 425-600 nm) as well as the recovery of **1a**-**1d** (λ 350-425 nm); (ii) all photoproducts reacted efficiently with tetracyanoethylene (TCNE), an excellent hydride acceptor (Figures S4-S5),[41] producing the corresponding naphthoxanthenium cations in polar solvents (Figure S6). This confirms the presence of a weak C(sp^3)-H bond in the photoproducts, in agreement with the calculations for the proposed NXs (Table S1).

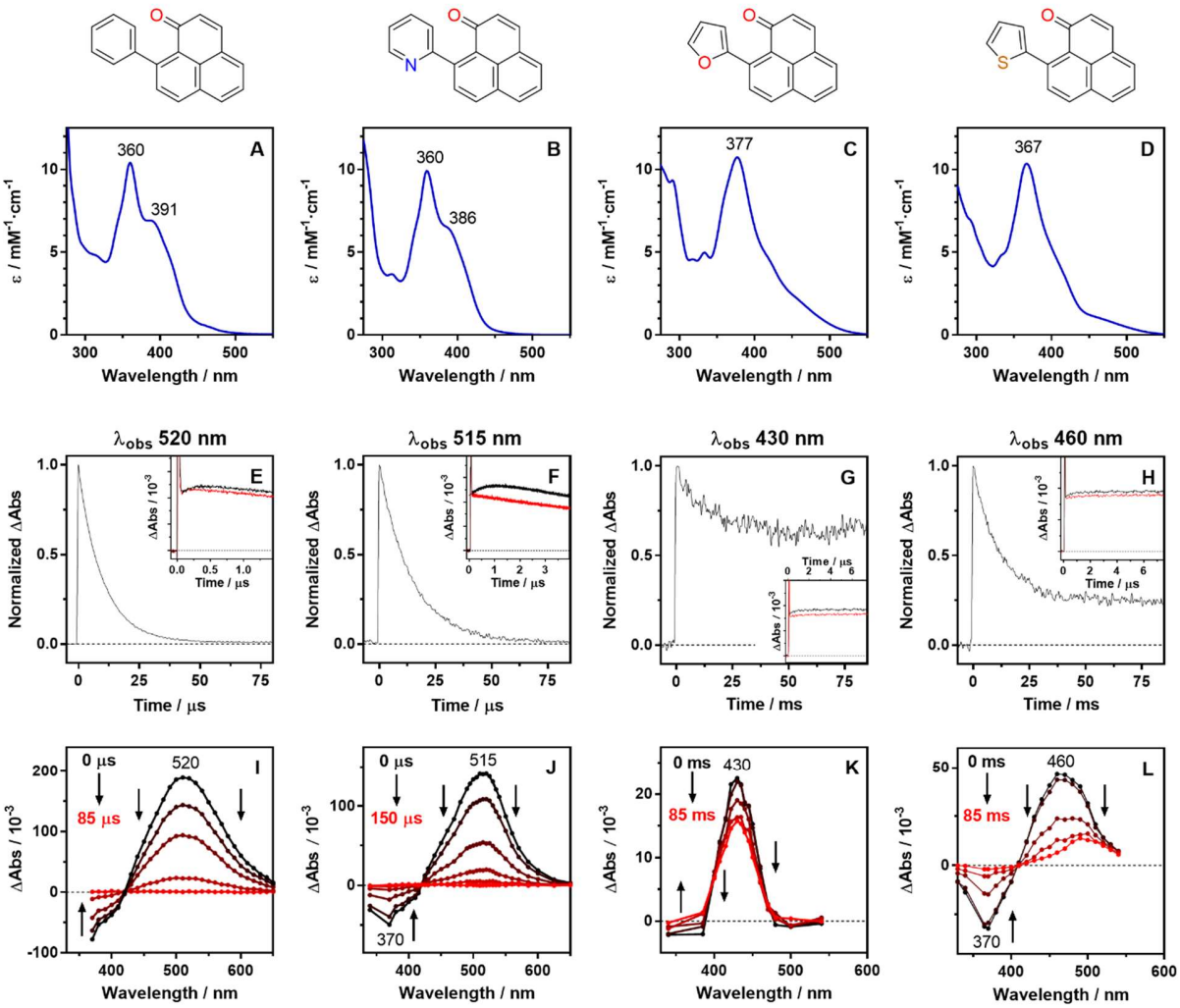

Figure 1. Photophysical characterization of **1a** (A,E,I), **1b** (B,F,J), **1c** (C,G,K), **1d** (D,H,L) in acetonitrile; λ_{exc} = 355 nm. (A-D): Absorption spectra. (E-H): **2a-2d** Transient absorption traces in argon-saturated solvent (black line). Inset: Detail of the naphthoxanthene formation kinetics under argon (black line) and air (red line). (I-L): Time evolution of the transient absorption spectra.

The kinetics of NX production in **1a-1d** were biphasic (Figure 1, panels E-H inset), showing a fast-initial spike and a slower rise, which indicates that the NXs are formed from both their singlet and triplet states. Consistent with this, the triplet lifetimes, deduced from the slow-rise component, were more than 50-fold shorter than that of the unsubstituted phenalenone (PN), which cannot undergo photocyclization (Table S1). Moreover, the slow rise component disappeared upon aeration (Figure 1, panels E-H) and production of singlet oxygen was observed (Table S1 and Figure S7), indicating efficient oxygen quenching of the triplet state. The decay of the NX form was insensitive to oxygen but its lifetime was strongly affected by the nature of the arylic substitution at position C-9, increasing from a few microseconds for **2a,b** to tens of milliseconds for **2c**,**2d**. The trend is in concordance with the measured activation energy for ring-opening (Table S1 and Figure S8). Of note, the decay of **2c** and **2d** (panels K and L, respectively) does not completely restore the initial concentration of **1c** and **1d**. In addition, the transient spectrum of **2d** (panel L) showed a spectral evolution over the course of its decay. We show below that these observations are consistent with the formation of *ipso- and ortho-adducts addition* for these specific compounds.

Strikingly different observations could be made for **1e** (Figure 2). Nanosecond laser flash photolysis also showed a long-lived transient (Figure 2C) but, unlike those derived from **1a-1d**, it could be quenched by oxygen (from 50 μs in argon-saturated PBS solutions to 2 μs upon aeration; k_q = 3x10^9 M^{-1}s^{-1}) and is therefore assigned to a triplet state. For comparison, the triplet lifetime of the unsubstituted PN is 38 μs.[42] The quantum yield of singlet oxygen production ($\Phi_\Delta = 0.08$) is comparable to those of **1a-1d** (Φ_Δ = 0.02-0.16, Table S1) and much smaller than that of the unsubstituted PN (Φ_Δ =1).[42-44] Thus, we hypothesized that **1e** is also able to produce the NX photoisomer **2e**, albeit in shorter time scales. We investigated this possibility using femtosecond transient absorption spectroscopy. Figure 2D shows that the femtosecond time-resolved spectra, recorded in air-saturated PBS solutions, evolved from a maximum at 585 nm to 540 nm within

300 ps. The spectrum of the latter species is very similar to that of the triplet state of **1e**, as measured by nanosecond laser flash photolysis (535 nm, Figure 2E) and is also very similar to that of triplet PN.[42,45] Global analysis revealed a very fast rise component (4.4 ps), followed by a fast (70 ps) and a slow decay component (Figure 2B). The slow component corresponds to the triplet state and therefore was fixed to 2 microseconds in our analysis, as extracted from the nanosecond laser flash photolysis data in Figure 2C. On the other hand, the spectrum of the 70-ps component matches the calculated spectrum for **2e** (maximum at 585 nm and 578 nm, respectively; Figures S9 and S10). Finally, the 4.4 ps lifetime is assigned to the **1e** singlet excited by comparison with the lifetime of singlet PN (29 ps),[31] the seven-fold shortening indicating the operation of new, very efficient deactivation processes, which we ascribe to photocyclization. For comparison, the lifetime of singlet **1a** is 13 ps.[31] The results above suggest that the major pathway for the **1e** singlet excited-state deactivation is photocyclization to **2e**, effectively competing with intersystem crossing to the triplet state. Judging from the decrease of both the singlet lifetime and of the singlet oxygen quantum yield (which is an upper-limit value of the intersystem-crossing quantum yield), compared to those of PN, we estimate that ~90% of the singlet **1e** undergo photocyclization. Finally, the observation that the triplet state lives 50 μs in argon-saturated solutions, a value comparable to the lifetime of triplet PN, rules out any significant photocyclization from the triplet state, a major difference from compounds **1a-1d**.

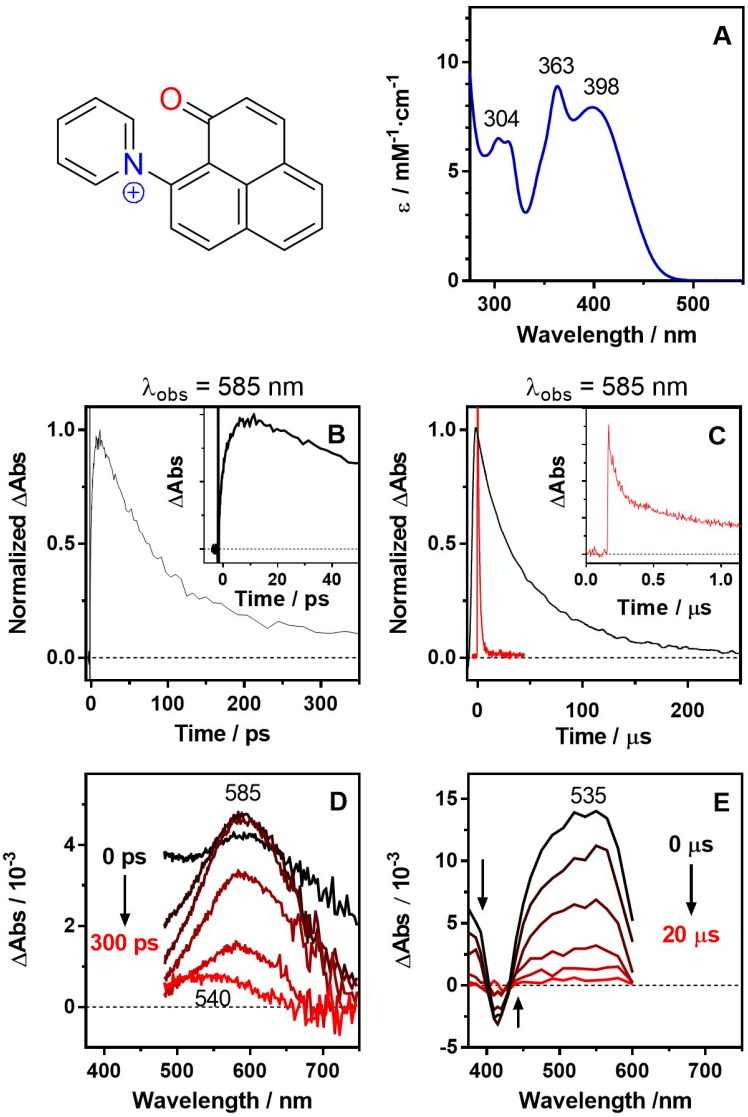

Figure 2. Photophysical characterization of **1e** in PBS (pH 7.4); λ_{exc} = 387 nm. (A): Absorption spectra. (B): Femto- and (C) nanosecond transient absorption kinetics in argon- and air-saturated PBS (black and red line respectively). Insets: Detail of the transient formation kinetics. (D, E) Evolution of the transient absorption spectra in the pico- (D) and microsecond (E) timescales.

2.2 Computational Calculations

Theoretical calculations provide support and further insights for the above observations. The excited-state pathway for ring closure in **1a** is the addition of the ketone moiety to the *ortho*-

position of the 9-phenyl-ring (**2a**), whereas *ipso*-addition suffers from endothermicity and a concomitant higher barrier, as reported previously.[23] For the 2-pyridyl derivative **1b**, a novel situation arises in that the aromatic substituent on the phenalenone system no longer has a plane of symmetry. In principle, *ortho*-addition can take place to two sides of the pyridine ring, and there are two rotamers of the ketone (red and grey lines in Figure 3). The calculations show that addition to the 3-position of the pyridine ring (**2b**) should be the preferred site of attack. *Ipso*-addition (**2b'**) is predicted to be hindered by a large barrier, which is unsurprising, as this position is very electron-poor. Addition to the pyridine N (**2b''**; red line in Figure 3) is predicted to have a fairly small barrier. However, this reaction pathway is both endothermic and endergonic, and therefore unlikely to be of any significance. What is remarkable about this system is the fact that **2b''** appears to have a triplet ground state, which may be due to some degree of antiaromaticity, as the middle top ring has eight π-electrons. This antiaromaticity is probably also reflected in the fairly high barrier calculated for the ring-opening of singlet **2b''**. The kinetics of ring-opening of **2b** is predicted to be similar to that of **2a** (black line in Figure 3).

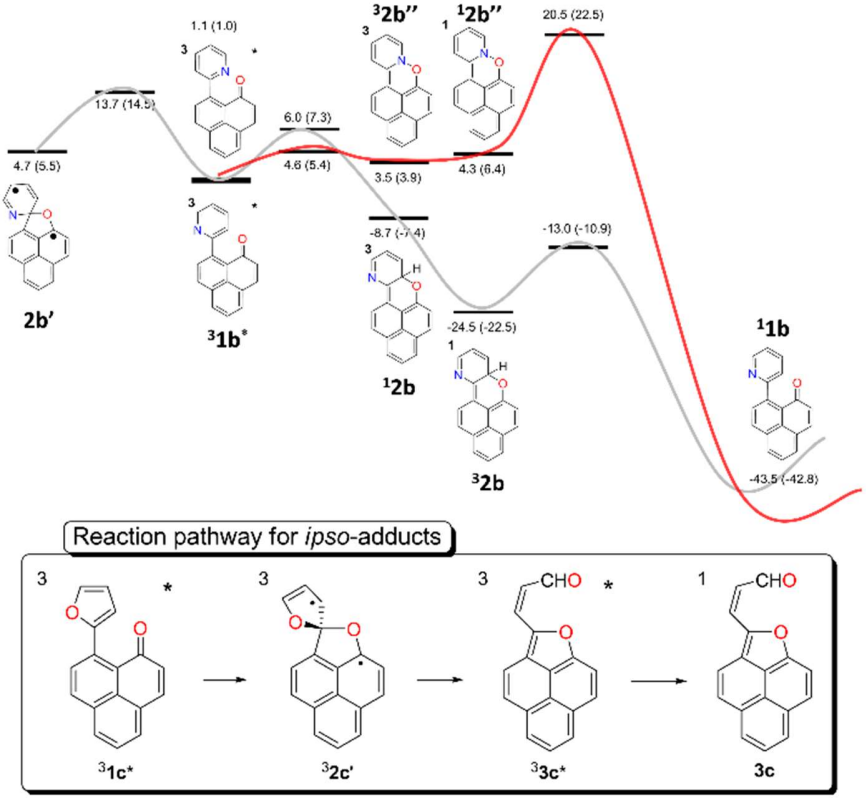

Figure 3. Top: Reaction pathways after triplet excitation of **1b**. Energies (without brackets) and Gibbs free energy (brackets), as calculated at the ((U)M05-2X/cc-pVTZ) level of theory, are given in kcal/mol relative to the triplet state. Solid lines connecting the different states are provided as a visual aid only. Bottom: Pathways of ipso-adduct decay in **2c**.

For the *ipso*-addition, there is only one TS, in which the two ring systems are perpendicular to each other. Coming from the *ipso*-biradical, the system therefore will have to pass a valley-ridge-inflection point to bifurcate to either the *syn*- or *anti*-conformer of the ketone triplet. This also holds for the other heterocyclic systems.

In the case of the 2-substituted 5-membered heterocycles, again the presence of two different rotamers of the ketones has to be considered (Figure S11). However, addition can only take place to one side, as addition to the heteroatom appears to be an unlikely option. The barrier for ring-opening of **2c** and **2d** is predicted to be on the order of 18 kcal mol^{-1}, which is significantly higher than that of **2a-b**, resulting in millisecond range lifetimes for **2c,d**. Unlike the phenyl- and pyridyl-substituted derivatives, *ipso*-addition is predicted to be considerably faster than *ortho*-addition for **1c**, while it should be similarly fast for **1d**. To our delight, the transient absorption results are consistent with these predictions (Figure 1 panels G,H): the transient initially assigned to **2c,d** contains, in fact, two components, which, in the light of the calculations, we assign to the transient *ortho*-adducts (**2c,d**, shorter-lived) and products (**3c**, **3d**, lifetime in excess of 100 ms) derived from *ipso*- (**2c',d'**) adducts. Thus, the *ipso*-pathway is favoured in the furyl derivative (larger amplitude) but the *ortho*- in the thienyl one (smaller amplitude). Calculated UV/Vis spectra corroborate the assignment of the residual absorption observed upon LFP of **1c** and **1d** to aldehyde **3c** and thioaldehyde **3d**, with excellent agreement between the residual absorption in Figure 1K / 1L and the calculated spectra of **3c** / **3d** (see Figures S12 and S13).

Ipso-addition has been previously observed for triplet β-phenylpropiophenone, where it is the main decay pathway.[40,46-50] The intermediate biradical formed in this system is very short-lived (< 20 ps) and deactivates back to the starting material. The results of our experiments and calculations indicate a possible different outcome for the corresponding biradicals **2c'** and **2d'**. Specifically, formation of stable photoproducts, e.g. **3c** (Figure 3), can be expected for these molecules, which is consistent with the trend in photostability **1c** < **1d** << **1b** < **1a** (Figure S14).

Formation of **3c** from ^{3}**1c*** is exergonic by ΔG = -33.6 kcal mol^{-1} but should be slow because the calculated free energy of activation for ring-opening of ^{3}**2c'** to ^{3}**3c*** is quite significant in the gas phase ($\Delta G^{\ddagger}$ = 19.5 kcal mol^{-1}). However, a surface-crossing mechanism, yielding ground-state **3c** directly from ^{3}**2c'** might explain the formation of **3c.** Or **3c** is directly formed from **1c** on the singlet excited state surface. Attempts to isolate the photoproducts failed but we have obtained a compound very similar to **3c** from the reaction of 9-trifluoromethanesulfonyloxy-phenalenone with sodium azide.[51]

Striking differences set the derivative **1e** apart from **1a-1d**: Transient absorption experiments (Figure 2) indicate that **2e** is produced only from the singlet excited state, while the triplet state yields exclusively singlet oxygen. Consistent with these observations, theoretical calculations indicate that **2e** production from the triplet state is unlikely due to a very high activation energy (Figure S15). On the other hand, the barrier for electrocyclic ring-opening of **2e** is calculated to be 4-5 kcal mol^{-1}, significantly smaller than for **1a** (ca. 10 kcal mol^{-1}), which is consistent with the 70 ps lifetime observed for **2e**. Such ultrafast (~ 14 GHz) oscillation rate is ideal for high-end optical switching applications.

2.3 Discussion

The significance of the results can be gauged in the light of the biological role of 9-phenylphenalenones, which participate in plant defense against pathogen infections, either directly or through the production of coloured naphthoxanthene secondary metabolites.[25-27] The study of such a process led us to the discovery of a thermally-reversible photocyclization reaction to produce metastable naphthoxanthenes.[22-24] The current work demonstrates that this reversible photochromism can be extended to phenalenones substituted with heteroaryl moieties such as pyridyl, furyl, thienyl, and pyridinium. The loss of local aromaticity in the closed forms is the driving force for the ring-opening reaction. Thus, by modulating the electronic nature of the aryl group at position C-9, it is possible to fine-tune the lifetime of the closed-ring isomer over nine orders of magnitude, from tens of picoseconds to tens of milliseconds. The theoretical insights gained suggest that further widening of this time span is possible.

It is interesting to note that the photocyclization and subsequent thermal ring-opening in 9-aryl-phenalenones share many similarities with the photoisomerization process of chromenes (e.g., naphthopyrans, benzo[b]chromenes or oxazines among others; Scheme 2) but, surprisingly, the process occurs in the opposite direction.[52-55] The stable isomer in chromenes is the closed-form (**1f**), which undergoes ring opening to the less stable α,β,γ,δ-unsaturated ketone (**2f**) upon photoirradiation. Close inspection of the structure of **2f** reveals that the reverse reaction is a cycloaddition between the carbonyl and the newly-formed vinyl group in the β-position, which is very similar to the photocyclization reaction in 9-aryl-phenalenones.

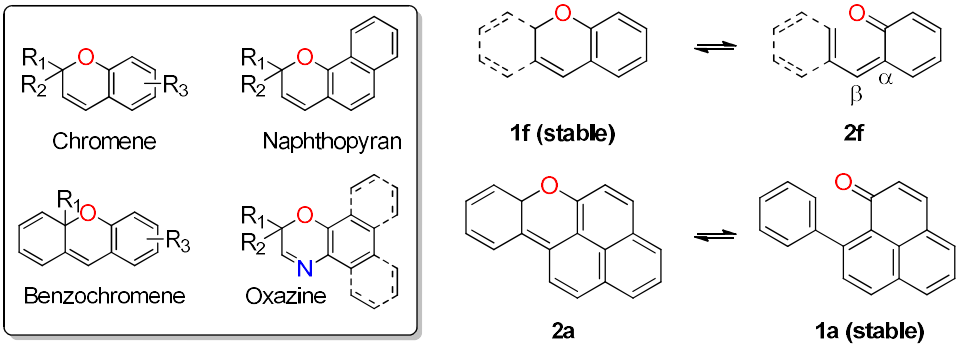

Scheme 2. Left: Representative structures of the different families of chromenes. Right: Reaction pathway for 2H-chromene core (**1f**) and 9-phenylphenalenone (**1a**).

It can therefore be postulated that 9-aryl-phenalenones can be considered as "inverted-chromenes", in which the open form is more stable because the local aromaticity of the phenalenone and the aryl substituent is preserved. In contrast, it is the closed structure of chromenes that preserves the aromaticity of the system,[52,56] even when it contains vinyl- or aryl-β-substituents.[57] Interestingly, the open form of 12a*H*-12a-methylnaphtho[3,2]chromene has been reported to undergo a photocycloaddition reaction yielding the *ipso* adduct.[58,59]

3. Conclusions

In summary, photoexcitation of a series of bioinspired 9-arylphenalenones (**1a**-**1e**) leads to the formation of their corresponding naphthoxanthenes (**2a**-**2e**), which thermally revert to the original 9-arylphenalenones (**1a**-**1e**) with time constants ranging from ultrafast (picoseconds) to milliseconds depending on the electronic density of the aryl substituent. The results obtained

provide a sound basis for the development of 9-aryl-phenalenones as a new family of thermally reversible photochromic compounds. Of specific interest, compound **1e**, with an oscillation frequency ~ 14 GHz, shows strong promise for ultrafast photoswitching applications.

4. Experimental Section

4.1 Materials

1a-e were synthesized as described elsewhere.[25,51,60] PN was purchased from Sigma-Aldrich (St Louis, USA) and used without further purification. All solvents used were of spectroscopic quality or higher and were purchased from Scharlab (Sentmenat, Spain) or Sigma-Aldrich (St Louis, USA). To change oxygen concentration in the solution, a stream of oxygen 5.0 or argon 5.0 (Carburos Metálicos, Cornellà de Llobregat, Spain) was flowed above the sample solution under gentle stirring for 20 minutes.

4.2 General spectroscopic measurements

UV-Vis spectra were recorded with a Varian Cary 6000i spectrometer (Varian, Palo Alto, USA). Nanosecond transient absorption kinetics and spectra were monitored by nanosecond laser flash photolysis using a Surelite I-10 Continuum Q-switched Nd:YAG laser operated at the third harmonic (355 nm; Continuum, San Jose, USA) with right-angle geometry and an analyzing beam produced by a 75 W Xe lamp (PTI, Birmingham, USA) in combination with a dual-grating PTI-101 monochromator (PTI, Birmingham, USA) coupled to a PTI-710 UV-Vis radiation detector (PTI, Birmingham, USA). The signal was fed to a Lecroy WaveSurfer 454 oscilloscope (Lecroy Corporation, New York, USA) for digitizing and averaging (typically between 10 to 100 shots) and finally transferred to a PC for data storage and analysis.

Femtosecond transient absorption kinetics and spectra were recorded in a homebuilt system at IMDEA Nanoscience in Madrid, in which a Clark-MXR (CPA-2101) system (driven at 1 kHz by a regenerative amplifier) provided a 775 nm femtosecond laser pulse. One fraction of it is sent to a supercontinuum generator (SCG—a sapphire plate) to generate white light from 477 nm to 1600 nm and used as the probe pulse. Before reaching the sample, a fraction of the probe pulse is taken to form the reference pulse to reduce the laser fluctuation induced noise in the signal. The other fraction of the 775 nm femtosecond pulse is converted into a 387 nm pump pulse by a second harmonic generator (SHG), chopped at 500 Hz with a mechanical chopper, and used for

sample excitation. Pump-probe delays up to 500 ps, with 150 fs time resolution, are achieved by delaying the pump pulse with a mechanical translation stage. The spot sizes of the pump and probe pulses on the sample are 260 µm and 130 µm, respectively. The pump pulse is blocked after passing through the sample, while the probe and reference probe pulses are detected via a prism spectrometer (Entwicklungsbüro Stresing GmbH) consisted of a dual-channel CCD array (2 x 256 pixels, VIS-enhanced InGaAs, Hamamatsu Photonics Inc.). The residual fundamental 775 nm pulse is removed by a notch filter. Neutral density filters are used to regulate both pump and probe pulse intensities and half lambda plates for their polarization angles. Data acquisition and data analysis, including global spectral modeling of the TA spectra, are accomplished by a custom-built Python program based on open source packages (Matplotlib, PyQt4, Scipy, Pyserial, etc.).

For irradiation and photostability studies were performed using a Surelite I-10 Continuum Q-switched Nd:YAG laser operated at the third harmonic (355 nm and 10 mJ per pulse/cycle).

Production of singlet oxygen ($^1O_2$) was studied by time-resolved near-infrared phosphorescence at 1275 nm as described in previous works.[61,62] A pulsed Nd:YAG laser (FTSS355-Q, Crystal Laser, Berlin, Germany) working at 355 nm (1 kHz; third harmonic; 0.5 µJ per pulse) was used for sample excitation. A 1064 nm rugate notch filter (Edmund Optics) and an uncoated SKG-5 filter (CVI Laser Corporation) were placed at the exit port of the laser to remove any residual component of its fundamental emission in the near-infrared region. The luminescence exiting from the sample was filtered by an 1100 nm long-pass filter (Edmund Optics) and a narrow bandpass filter at 1275 nm (BK-1270-70-B, bk Interferenzoptik). A thermoelectric-cooled near-infrared sensitive photomultiplier tube assembly (H9170-45, Hamamatsu Photonics) was used as detector. Photon counting was achieved with a multichannel scaler (NanoHarp 250, PicoQuant). The time dependence of the $^1O_2$ phosphorescence with the signal intensity S(t) is described by Eq. 1, where τ_T and τ_Δ are the lifetimes of the photosensitizer triplet state and $^1O_2$, respectively, and S(0) is a quantity proportional to Φ_Δ.

$$S(t) = S(0)\frac{\tau_\Delta}{\tau_\Delta - \tau_T}\left(e^{\frac{-t}{\tau_\Delta}} - e^{\frac{-t}{\tau_T}}\right) \qquad Eq.1$$

Thus, Φ_{Δ} was determined by comparing the S(0) values of optically-matched solutions of the sample and a suitable reference at 355 nm as described by Eq. 2. The references chosen are phenalenone ($\Phi_{\Delta;\text{benzene}}$ = 0.92 ± 0.03; $\Phi_{\Delta;\text{acetonitrile}}$ = 1.00 ± 0.03)[42-44] and sodium 1H-phenalen-1-one-2-sulphonate (PNS; $\Phi_{\Delta;PBS}$ = 0.97 ± 0.06).[63]

$$\phi_{\Delta,drug} = \frac{S(0)_{drug}}{S(0)_{reference}} \phi_{\Delta,reference} \qquad Eq. 2$$

4.3 Computational methods

All calculations were performed employing the Gaussian09 suite of programs.[64] Stationary points were fully optimized at the M05-2X/cc-pVTZ level of theory,[65,66] and characterized as minima or transition structures by performing a vibrational analysis. In some cases, the influence of solvation on structures and energies was taken into account by employing a polarizable continuum model.[67,68]

Supporting Information

Supplementary data to this article can be found online at xxx.

Reactivity of **2a**-**2d** towards TCNE. Calculated UV-Vis absorption spectra for **2b**-**2e** and **3c**,**3d**. Singlet oxygen quantum yield determination for **1a**-**1e**. Arrhenius plots for **2a**-**2d**.Calculated photoreaction pathways for **1c**-**1e**. Photostability studies for **1a**-**1d**. Cartesian coordinates and electronic energies for all the calculated species. (PDF)

Abbreviations

BPQ	β-phenyl quenching
NX	Naphthoxanthene
PBS	Phosphate buffer saline (pH 7.4)
PN	Phenalenone
TCNE	Tetracyanoethylene
TS	Transition state
$^1O_2$	Singlet oxygen
9PPNs	9-Phenylphenalenones
Φ_Δ	Singlet oxygen generation quantum yield
τ	Lifetime

Author Contributions

All authors discussed the results and commented on the manuscript. All authors have approved the final version of the manuscript.

Notes

The authors declare no competing financial interest.

ACKNOWLEDGMENT

Dedicated to the memory of Josep Obach Calafell (1929-2019). This work has been supported by grant CTQ2016-78454-C2-1-R from the Spanish Ministerio de Economía y Competitividad. R. B.-O. thanks the European Social Funds and the SUR del DEC de la Generalitat de Catalunya for a predoctoral fellowship (2017 FI_B2 00140) and the Vlaanderen Fonds Wetenschappelijk Onderzoek (grant number 12Z8120N). Support from the Severo Ochoa Excellence program for IMDEA Nanociencia is acknowledged (SEV-2016-0686).

Bibliography

(1) Vaia, R.; Baur, J. Adaptive Composites *Science* **2008**, 319, 420-421.

(2) Mayer, G.; Heckel, A. Biologically Active Molecules With a "Light Switch" *Angew. Chem. Int. Ed.* **2006**, 45, 4900–4921.

(3) Szymański, W.; Beierle, J.M.; Kistemaker, H.A.V; Velema, W.A.; Feringa, B.L. Reversible Photocontrol of Biological Systems by the Incorporation of Molecular Photoswitches. *Chem. Rev.* **2013**, 113, 6114–6178.

(4) Broichhagen, J.; Frank, J.A.; Trauner, D.A. Roadmap to Success in Photopharmacology *Acc. Chem. Res.* **2015**, 48, 1947–1960.

(5) Bléger, D.; Hecht, S. Visible-Light-Activated Molecular Switches *Angew. Chem. Int. Ed.* **2015**, 54, 11338-11349.

(6) Irie, M. Diarylethenes for Memories and Switches *Chem. Rev.* **2000**, 100, 1685–1716.

(7) Heilemann, M.; Dedecker, P.; Hofkens, J.; Sauer, M. Photoswitches: Key Molecules for Subdiffraction-Resolution Fluorescence Imaging and Molecular Quantification. *Laser Photonics Rev.* **2009**, 3, 180–202.

(8) El Gemayel, M.; Börjesson, K.; Herder, M.; Duong, D.T.; Hutchison, J.A.; Ruzie, C.; Schweicher, G.; Salleo, A.; Geerts, Y.; Hecht, S.; Orgiu, E.; Samori, P. Optically Switchable Transistors by Simple Incorporation of Photochromic Systems into Small-Molecule Semiconducting Matrices. *Nat. Commun*. **2015**, 6, 6330.

(9) Smaali, K.; Karpe, S.; Blanchard, P.; Deresmes, D.; Godey, S.; Rochefort, A.; Roncali, J.; Vuillaume, D.; Hc, C. High On-Off Conductance Switching Ratio in Optically-Driven Self-Assembled Conjugated Molecular Systems. *ACS Nano* **2010**, *4*, 2411–2421.

(10) Mustroph, H.; Stollenwerk, M.; Bressau, V. Current Developments in Optical Data Storage with Organic Dyes. *Angew. Chem. Int. Ed.* **2016**, *45*, 2016–2035.

(11) Venkataramani, S.; Jana, U.; Dommaschk, M.; Sönnichsen, F.D.; Tuczek, F.; Herges, R. Magnetic Bistability of Molecules in Homogeneous Solution at Room Temperature. *Science* **2013**, *331*, 445–448.

(12) Jin, C.; Yan, R.; Huang, J. Cellulose Substance with Reversible Photo-Responsive Wettability by Surface Modification. *J. Mater. Chem.* **2011**, *21*, 17519–17525.

(13) Bouas-Laurent, H.; Dürr, H. Organic Photochromism. *Pure Appl. Chem.* **2001**, *73*, 639–665.

(14) García-Amorós, J.; Velasco, D. Recent Advances Towards Azobenzene-Based Light-Driven Real-Time Information-Transmitting Materials. *Beilstein J. Org. Chem.* **2012**, *8*, 1003–1017.

(15) Waldeck, D.H. Photoisomerization Dynamics of Stilbenes. *Chem. Rev.* **1991**, *91*, 415–436.

(16) Shima, K.; Mutoh, K.; Kobayashi, Y.; Abe, J. Enhancing the versatility and functionality of fast photochromic bridged imidazole dimers by flipping imidazole rings. *J. Am. Chem. Soc*. **2014**, *136*, 10, 3796–3799

(17) Beaujean, P.; Bondu, F.; Plaquet A.; Garcia-Amorós, J.; Cusido, J.; Raymo, F.M.; Castet, F.; Rodriguez, V.; Champagne, B. Oxazines: a new class of second-order nonlinear optical switches. *J. Am. Chem. Soc.* **2016**, *138*, 5052–5062.

(18) Kobayashi, Y.; Mutoh, K.; Abe, J. Fast photochromic molecules toward realization of photosynergetic effects. *J. Phys. Chem. Lett.* **2016**, *7*, 3666−3675.

(19) Boelke, J.; Hecht, S. Designing Molecular Photoswitches for Soft Materials Applications *Adv. Opt. Mat.* **2019**, 7, 1900404.

(20) Kitagawa, D.; Nakahama, T.; Nakai, Y.; Kobatake, S. 1,2-Diarylbenzene as Fast T-Type Photochromic Switch *J. Mater. Chem. C.* **2019**, 10, 2865-2870.

(21) Garcia-Amorós, J.; Maerz, B.; Reig, M.; Cuadrado, A.; Blancafort, L.; Samoylova, Dr.; Velasco, D.; Picosecond Switchable Azo Dyes *Chem. Eur. J.* **2019**, *25*, 7726-7732.

(22) Anamimoghadam, O.; Symes, M.D.; Busche, C.; Long, D.L.; Caldwell, S.T.; Flors, C.; Nonell, S.; Cronin, L.; Bucher, G. Naphthoxanthenyl, a New Stable Phenalenyl Type Radical Stabilized by Electronic Effects. *Org. Lett.* **2013**, *15*, 2970–2973.

(23) Bucher, G.; Bresolí-Obach, R.; Brosa, C.; Flors, C.; Luis, J.G.; Grillo, T.A.; Nonell, S. β-Phenyl Quenching of 9-Phenylphenalenones: A Novel Photocyclisation Reaction with Biological Implications. *Phys. Chem. Chem. Phys.* **2014**, *16*, 18813-18820.

(24) Bresolí-Obach, R.; Nonell, S. A Modern View on the Beta Phenyl Quenching of Aromatic Ketones. *Afinidad* **2016**, *73*, 90-95.

(25) Luis, J.G.; Fletcher, W.Q.; Echeverri, F.; Grillo, T.A. Phenalenone-Type Phytoalexins from Musa Acuminata Synthesis of 4-Phenyl-Phenalenones. *Tetrahedron* **1994**, *50*, 10963–10970.

(26) Otálvaro, F.; Nanclares, J.; Vásquez, L.E.; Quiñones, W.; Echeverri, F.; Arango, R.; Schneider, B. Phenalenone-Type Compounds from Musa Acuminata Var. "Yangambi Km 5" (AAA) and their Activity Against *Mycosphaerella Fijiensis*. *J. Nat. Prod.* **2007**, *70*, 887–890.

(27) Flors, C.; Nonell, S. Light and Singlet Oxygen in Plant Defense Against Pathogens: Phototoxic Phytoalexins. *Acc. Chem. Res.* **2006**, *39*, 293–300.

(28) López-Arencibia, A.; Reyes-Batlle, M.; Freijo, M.B.; McNaughton-Smith, G.; Martín-Rodríguez, P.; Fernández-Pérez, L.; Sifaoui, I.; Wagner, C.; García-Méndez, A.B.; Liendo, A.R.; Bethencourt-Estrella, C.J.; Grillo, T.A.; Piñero, J.E.; Lorenzo-Morales, J. In Vitro Activity of 1*H*-Phenalen-1-One Derivatives Against *Acanthamoeba Castellanii* Neff and their Mechanism of Cell Death. *Exp. Parasitol.* **2017**, *183*, 218-223.

(29) Edwards, J.M.; Weiss U. Phenalenone Pigments of the Root System of *Lachnanthes tinctoria Phytochemistry* **1974**, 13, 1597-1602.

(30) Lazzaro, A.; Corominas, M.; Martí, C.; Flors, C.; Izquierdo, L.R.; Grillo, T.A.; Luis, J.G.; Nonell, S. Light- and Singlet Oxygen-Mediated Antifungal Activity of Phenylphenalenone Phytoalexins. *Photochem. Photobiol. Sci.* **2004**, *3*, 706–710.

(31) Flors, C.; Ogilby, P.R.; Luis, J.G.; Grillo, T.A.; Izquierdo, L.R.; Gentili, P.L.; Bussotti, L.; Nonell, S. Phototoxic Phytoalexins. Processes that Compete with the Photosensitized Production of Singlet Oxygen by 9-Phenylphenalenones. *Photochem. Photobiol*. **2006**, *82*, 95–103.

(32) Song, R.; Feng, Y.; Wang, D.; Xu, Z.; Li, Z.; Shao, X. Phytoalexin Phenalenone Derivatives Inactivate Mosquito Larvae and Root-knot Nematode as Type-II Photosensitizer *Sci. Rep.* **2017**, 7, 42058.

(33) Cooke, R.; Dagley, I. Colouring Matters of Australian Plants. XXI. Naphthoxanthenones in the *Haemodoraceae Aust. J. Chem.* **1979**, 32, 1841–1847.

(34) Opitz, S.; Holscher, D.; Oldham, N.J.; Bartram, S.; Schneider, B. Phenylphenalenone-Related Compounds: Chemotaxonomic Markers of the *Haemodoraceae* from Xiphidium caeruleum *J. Nat. Prod.* **2002**, 65, 1122–1130.

(35) Duque, L.; Zapata, C.; Rojano, B.; Schneider, B.; Otálvaro, F. Radical Scavenging Capacity of 2,4-Dihydroxy-9-phenyl-1H-phenalen-1-one: A Functional Group Exclusion Approach *Org. Lett.* **2013**, 15, 3542-3545.

(36) Butler, D. Fungus Threatens Top Banana *Nature* **2013**, 504, 195–196.

(37) Hidalgo, W.; Chandran, J.N.; Menezes, R.C.; Otálvaro, F.; Schneider, B. Phenylphenalenones Protect Banana Plants from Infection by *Mycosphaerella fijiensis* and are Deactivated by Metabolic Conversion *Plant Cell Environ.* **2016**, 39, 492-513.

(38) Bucher, G. Interaction of Triplet Excited States of Ketones with Nucleophilic Groups: (π,π*) and (n,π*) versus (σ*,π*) States. Substituent-Induced State Switching in Triplet Ketones *Aust. J. Chem.* **2017**, 70, 387-396.

(39) Bresolí-Obach, R.; Gispert, I.; Peña, D.G.; Boga, S.; Gulias, O.; Agut, M.; Vázquez, M.E.; Nonell, S. Triphenylphosphonium Cation: A Valuable Functional Group for Antimicrobial Photodynamic Therapy *J. Biophotonics.* **2018**, 11, e201800054.

(40) Bucher, G. Addition of the Carbonyl Oxygen to the Ipso- or Ortho-Carbon Atoms of the Beta-Phenyl Ring Followed by Intersystem Crossing and Rapid Relaxation to the Ground-State Ketones: A Mechanism for β-Phenyl Quenching of the First Triplet Excited States of Derivatives of β-Phenylpropiophenone. *J. Phys. Chem. A* **2008**, *112*, 5411–5417.

(41) Dhar, D.N. The Chemistry of Tetracyanoethylene *Chem. Rev.* **1967**, *67*, 611–622.

(42) Oliveros, E.; Suardi-Murasecco, P.; Aminian-Saghafi, T.; Braun, A.M.; Hansen, H.J. 1*H*-Phenalen-1-One: Photophysical Properties and Singlet-Oxygen Production. *Helv. Chim. Acta* **1991**, *74*, 79–90.

(43) Schmidt, R.; Tanielian, C.; Dunsbach, R.; Wolff, C. Phenalenone, a Universal Reference Compound for the Determination of Quantum Yields of Singlet Oxygen $O_2(^1\Delta_g)$ Sensitization *J. Photochem. Photobiol. A: Chem.* **1994**, 79, 11-17.

(44) Marti, C.; Jürgens, O.; Cuenca, O.; Casals, M.; Nonell, S. Aromatic Ketones as Standards for Singlet Molecular Oxygen $O_2(^1\Delta_g)$ Photosensitization. Time-Resolved Photoacoustic and Near-IR Emission Studies *J. Photochem. Photobiol. A: Chem.* **1996**, 97, 11-18.

(45) Flors, C. Nonell, S. Radical Species Derived from Phenalenone: Characterization and Role of Upper Excited States *J. Photochem. Photobiol. A. Chem.* **2004**, 163, 9-12.

(46) Wagner, P.J.; Kelso, P.A.; Kemppainen, A.E.; Haug, A.; Graber, D.R. Deactivation of Ketone Triplets by β-Phenyl Substitution. *Mol. Photochem.* **1970**, *2*, 81–85.

(47) Wismontski-Knittel, T.; Kilp, T. Intramolecular Quenching of Carbonyl Triplets by β-Phenyl Rings. *J. Phys. Chem.* **1984**, *88*, 110–115.

(48) Netto-Ferreira, J.C.; Leigh, W.J.; Scaiano, J.C. Laser Flash Photolysis Study of the Photochemistry of Ring-Substituted β-Phenylpropiophenones. *J. Am. Chem. Soc.* **1985**, *107*, 2617–2622.

(49) Moorthy, J.N.; Monahan, S.L.; Sunoj, R.B.; Chandrasekhar, J.; Bohne, C. Modulation of Lifetimes and Diastereomeric Discrimination in Triplet-Excited Substituted Butane-1,4-diones through Intramolecular Charge-Transfer Quenching. *J. Am. Chem. Soc.* **1999**, *121*, 3093–3103.

(50) Samanta, S.; Mishra, B.K.; Pace, T.C.S.; Sathyamurthy, N.; Bohne, C.; Moorthy, J.N. β-Phenyl Quenching of Triplet Excited Ketones: how Critical is the Geometry for Deactivation? *J. Org. Chem.* **2006**, *71*, 4453–4459.

(51) Anamimoghadam, O.; Long, D.L.; Bucher, G. 9-Iodo-phenalenone and 9-Trifluoromethanesulfonyloxyphenalenone: Convenient Entry Points to New Phenalenones Functionalised at the 9-Position. Iodine-Carbonyl Interaction Studies by X-ray Crystallography. *RSC Adv.* **2014**, *4*, 56654–56657.

(52) Becker, R.S.; Michl, J. Photochromism of Synthetic and Naturally Occurring 2*H*-Chromenes and 2*H*-Pyrans. *J. Am. Chem. Soc.* **1966**, 5931–5933.

(53) Coelho, P.J.; Carvalho, L.M.; Abrantes, S.; Oliveira, M.M.; Oliveira-Campos, A. M.F.; Guglielmetti, R. Synthesis and Spectrokinetic Studies of Spiro[Thioxanthene-Naphthopyrans]. *Tetrahedron* **2002**, *58*, 9505–9511.

(54) Ahmed, S.A.; Tanaka, M.; Ando, H.; Iwamoto, H.; Kimura, K. Synthesis and Photochromism of Novel Chromene Derivatives Bearing a Monoazacrown Ether Moiety. *Eur. J. Org. Chem.* **2003**, *13*, 2437–2442.

(55) Zhao, W.; Carreira, E.M. One-Pot Synthesis of Novel Photochromic Oxazine Compounds. *Org. Lett.* **2011**, *13 (19)*, 1609–1612.

(56) Hu, M.; Kawauchi, S.; Satoh, M.; Komiyama, J.; Watanabe, J.; Kobatake, S.; Irie, M. Two-Photon Photochromism of Two Simple Chromene Derivatives. *J. Photochem Photobiol.* A **2002**, *150*, 131–141.

(57) Moorthy, J.N.; Venkatakrishnan, P.; Samanta, S.; Kumar, D.K. Photochromism of Arylchromenes: Remarkable Modification of Absorption Properties and Lifetimes of o-Quinonoid Intermediates. *Org. Lett.* **2007**, *9*, 919–922.

(58) Uchida, M.; Irie, M. Two-Photon Photochromism of a Naphthopyran Derivative. *J. Am. Chem. Soc.* **1993**, *115*, 6442–6443.

(59) Uchida, M.; Irie, M. Structural Properties Required for Two-Photon Photochromism of Pyran Derivatives. *Chem. Lett.* **1995**, *24*, 323–324.

(60) Rosquete, L.I.; Cabrera-Serra, M.G.; Piñero, J.E.; Martín-Rodríguez, P.; Fernández-Pérez, L.; Luis, J.G.; McNaughton-Smith, G.; Grillo, T.A. Synthesis and *in vitro* Antiprotozoal Evaluation of Substituted Phenalenone Analogues *Bioorg. Med. Chem.* **2010**, 18, 4530–4534.

(61) Nonell, S.; Braslavsky, S.E. Time-Resolved Singlet Oxygen Detection *Methods Enzymol.* **2000**, 319, 37–49.

(62) Jiménez-Banzo, A.; Ragàs, X.; Kapusta, P.; Nonell, S. Time-Resolved Methods in Biophysics. 7. Photon Counting vs. Analog Time-Resolved Singlet Oxygen Phosphorescence Detection *Photochem. Photobiol. Sci.* **2008**, 7, 1003–1010.

(63) Nonell, S.; González, M.; Trull, F. 1*H*-Phenalen-1-one-2-sulfonic Acid: An Extremely Efficient Singlet Molecular Oxygen Sensitizer for Aqueous Media *Afinidad* **1993**, 44, 445-450.

(64) Frisch, M.J. et al, Gaussian 09, Revision A.02. Wallingford CT. **2009**.

(65) Dunning, T.H. Gaussian Basis Sets for Use in Correlated Molecular Calculations. I. The Atoms Boron through Neon and Hydrogen *J. Chem. Phys.* **1989**, 90, 1007–1023.

(66) Zhao, Y.; Schultz, N.E.; Truhlar, D.G. Design of Density Functionals by Combining the Method of Constraint Satisfaction with Parametrization for Thermochemistry, Thermochemical Kinetics, and Noncovalent Interactions *J. Chem. Theory Comput.* **2006**, 2, 364–382.

(67) Miertuš, S.; Scrocco, E.; Tomasi, J. Electrostatic Interaction of a Solute with a Continuum. A Direct Utilization of AB Initio Molecular Potentials for the Prevision of Solvent Effects *Chem. Phys.* **1981**, 55, 117–129.

(68) Tomasi, J.; Mennucci, B.; Cammi, R. Quantum Mechanical Continuum Solvation Models *Chem. Rev.* **2005**, 105, 2999–3094.